Phase diagram and magnetic structure investigation of the fcc antiferromagnet HoB_{12}

A. Kohout,[1] I. Batko,[1,2] A. Czopnik,[3] K. Flachbart,[2] S. Matas,[1,2] M. Meissner,[1] Y. Paderno,[4] N. Shitsevalova,[4] and K. Siemensmeyer[1]

[1]*Hahn Meitner Institut, Glienicker Str. 100, D-14109 Berlin, Germany*

[2]*Centre of Low Temperature Physics, Institute of Experimental Physics, Slovak Academy of Sciences, SK-04353 Kosice, Slovakia*

[3]*Institute of Low Temperature and Structure Research, PAS, PL-50950 Wroclaw, Poland*

[4]*Institute for Problems of Material Science, NASU, UA-252680 Kiev, Ukraine*

(Received 5 November 2003; revised manuscript received 29 June 2004; published 15 December 2004)

We have investigated the magnetic structure of the fcc antiferromagnet HoB_{12} by magnetization and specific heat measurements on small single crystals prepared from natural elements and by neutron diffraction on isotopically enriched powder samples. Magnetization measurements up to 9 T show up to three magnetic phases in the B vs T phase diagram, depending on the orientation of the applied field. The specific heat in zero field exhibits a very steep increase at $T_N = 7.4$ K, but its maximum is reached only at a lower temperature. In applied magnetic field up to 8 T additional λ-like anomalies are observed which confirm the phase boundaries from the magnetization measurements. Powder neutron diffraction in zero magnetic field reveals an antiferromagnetic structure below T_N. The basic reflections can be indexed with $(1/2 \pm \delta\, 1/2 \pm \delta\, 1/2 \pm \delta)$, where $\delta = 0.035$, pointing to an incommensurate magnetic structure. In a field below 2 T (in the lowest-field magnetic phase) the principal reflections remain; in a higher magnetic field they become suppressed. Moreover, the magnetic background strongly decreases with applied field. The analysis of results shows that an amplitude-modulated, incommensurate structure likely represents the magnetic order of HoB_{12}. The very complex phase diagram of this compound can arise from the interplay between the RKKY and dipole-dipole interaction and/or from frustration effects in the fcc-symmetry lattice.

DOI: 10.1103/PhysRevB.70.224416 PACS number(s): 75.40.−s, 61.12.−q, 75.50.Ee

I. INTRODUCTION

Rare earth dodecaborides exhibit a variety of physical properties which result predominantly from the $4f$ shell occupancy of their rare earth ions. Thus YbB_{12} is an intermediate valence system showing features of van Vleck paramagnetism, TmB_{12}, ErB_{12}, HoB_{12}, and DyB_{12} are metals which order antiferromagnetically at low temperatures, and LuB_{12} with a fully occupied $4f$ shell is a metal which becomes superconducting below about 0.4 K (Refs. 1–5). All the dodecaborides crystallize in a NaCl-based fcc structure where the Na^+ ions are replaced by rare earth ions and the Cl^- ions by B_{12} cubo-octahedra or icosahedra. The links within B_{12} clusters and between these clusters are determined by strong covalent bonds which are responsible for the rigidity and high melting temperatures of the dodecaborides.[1,6] Theoretical studies of the electronic structure of tetra-, hexa-, and dodecaborides indicate that two valence electrons of each rare earth atom compensate the electron deficiency of the boron sublattice, thus realizing the maximum stability.[7–9] This electron transfer generates an ionic bonding between rare earth and boron clusters. Despite the approximate character of this model, the electrical properties of these materials seem to be qualitatively explicable. According to this model, borides with divalent rare earth cations should become semiconductors, while borides with trivalent rare earths (e.g., Lu, Tm, Er, Ho, Dy) are metals with one electron per rare earth atom in the conduction band. Recent results of experimental and theoretical investigations of the electronic structure of some dodecaborides can be found in Refs. 10–12. E.g., there it is shown that the Fermi surface of LuB_{12} exhibits two conduction bands: a lower one and an upper one. The lower band has a Fermi surface similar to that of noble metals; the Fermi surface of the upper one is simply connected and almost spherical.[12]

As regards the magnetic dodecaborides, it was shown that an indirect exchange interaction of the RKKY type is an dominating mechanism leading to the observed antiferromagnetic ordering.[5,13] There are, however, indications that the magnetic structure of some of them (above all of HoB_{12}) exhibit more complex features[14,15] which cannot be explained by the RKKY interaction alone. The crystalline electric field plays an important role in the understanding of magnetic properties of this material, at least above their Néel temperature T_N (Ref. 15). The direct dipole-dipole interaction, which prefers ferromagnetic ordering in this structure, can play an important role in the magnetic structure formation as well because of the large effective magnetic moment p_{eff} of the Ho^{3+} ions ($p_{eff} \cong 10.5\mu_B$), as shown in Ref. 5.

From this point of view HoB_{12} exhibits similarities with the ultralow-temperature nuclear spin systems of Cu and Ag (Refs. 16 and 17). On the structural side they share the frustrated fcc structure and the high localization of the moment. As for the noble metals, there is one valence electron in the conduction band, a likely explanation for the similarities in the band structure which in turn should be reflected in the range function of the RKKY interaction. Thus the relative strengths of the RKKY and dipolar interaction are expected to govern the magnetic ordering, and the theoretical concepts developed for the nuclear spin systems of noble metals[17,18] can be tested. In the case of a dominating RKKY interaction—provided that the band structure of the noble metals is applicable—the interaction should be close to the

Heisenberg case[18,19] and frustration effects could be important. With increasing magnetic moment the dipolar anisotropy should become more important and in a magnetic field a complex phase diagram is expected although the lattice symmetry is high. The series of RB_{12} (R=Tm, Er, Ho, Dy) therefore provides ideal model systems to investigate the role of the various interactions—the magnitude of the dipolar interaction increases from Tm to Dy—whereas the RKKY interaction should remain very similar over the series. An important difference to the experimental work on the nuclear ordering in noble metals Cu and Ag is that in the RB_{12} system a full experimental characterization is possible without the limitations inherent to nuclear magnetism studies at ultralow temperature.

We have started with HoB_{12} which represents a case of strong dipolar interaction. It should be comparable to the RKKY interaction and therefore resemble the nuclear spin ordering in Cu. This is supported by the experimental ratio between paramagnetic Curie Weiss temperature of −24 K and the Neél temperature of 7.4 K (Ref. 5) which is almost as large as in Cu with −200 nK vs 60 nK. The aim of the present work was the investigation of the magnetic structure and phase diagram of HoB_{12}. To reveal and identify the detailed magnetic structure of this material we have measured the magnetization and specific heat of single-crystalline samples prepared from natural elements and performed neutron diffraction measurements using isotopically enriched Ho $^{11}B_{12}$ powder.

II. EXPERIMENTAL DETAILS

The magnetization data were taken within 1.7 K and 400 K with a commercial superconducting quantum interference device (SQUID) magnetometer (Quantum Design) in fields up to 5.5 T and in a homemade high-field magnetometer which is based on a commercial dc SQUID system (LOT) in the temperature range 1.5–50 K in magnetic fields up to B=9 T. The specific heat was measured in the temperature range between 0.5 K and 14 K and in a magnetic field up to 8 T by the relaxation method using a commercial calorimeter (Oxford Instruments). Neutron diffraction measurements were carried out on the powder diffractometer E6 at the BER II in Berlin using a wavelength of 2.4 Å. Two different diffractometer configurations have been used: one with an open collimation to achieve stronger signals and another one with a 10′ collimation in front of the monochromator to yield better resolution. A 5-T cryomagnet with a variable-temperature insert was used to set the temperature and magnet field.

The process of sample preparation comprised the synthesis of dodecaborides by borothermic reduction of rare earth oxides in vacuum at 1800–2000 K, the compacting of the thus received powders by slip casting into rods, the sintering in vacuum at 2000 K, and the process of inductive zone melting. The HoB_{12} samples for magnetization and specific heat measurements were obtained in single-crystalline form and cut from the same batch in the form of oriented, rectangular slabs. All samples have been characterized by a Laue picture which has shown cubic symmetry from opposite sides of the slabs. For neutron diffraction measurements isotopically enriched Ho $^{11}B_{12}$ powder was used.

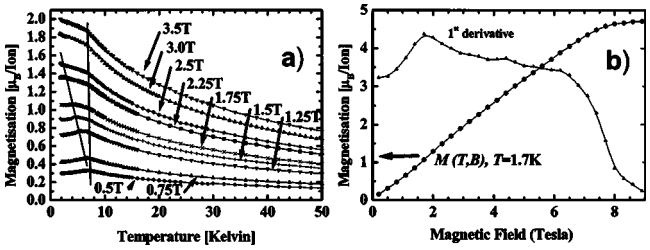

FIG. 1. (a) shows the magnetization of a HoB_{12} single crystal at different magnetic fields parallel to the (100) axis as a function of temperature. The solid lines indicate the onset and end of a plateau observed in the magnetization data which is associated with the phase boundaries between the paramagnetic, the AF1 and AF2 phases. (b) shows the field dependence measured on a polycrystalline sample at a constant temperature. The transition between the AF1 and AF2 phase is best seen in the derivative $\Delta M/\Delta B$ which was numerically estimated from the magnetization data.

III. EXPERIMENTAL RESULTS AND DISCUSSION

The typical temperature and field dependence of the magnetization $M(T)$ is shown in Fig. 1 for data obtained on an oriented single crystal and on a powder sample. In low magnetic field antiferromagnetic behavior is found; i.e., the magnetization decreases after a maximum is reached close to T_N. Towards lower temperature the magnetization does not approach zero; almost independent from the crystalline orientation, the magnetization extrapolates to approximately 70% of its maximum at T_N. Thus the magnetization data resemble the susceptibility from a powder sample with equal mixing of the transverse and longitudinal components of the susceptibility. In an intermediate magnetic field around 1 T and below T_N a linear regime of the magnetization is found, which gets broader with increasing field. In a magnetic field of 2.5 T below the ordering point this linear behavior prevails and no reduction of the magnetization is found down to 1.5 K.

As usual, the derivative of the magnetization with respect to temperature and, where appropriate, to the applied magnetic field has been used to define the phase boundaries. The corresponding phase diagrams obtained from oriented single crystals are displayed in Fig. 2 and indicate that three different magnetic structures (denoted as AF1, AF2, and AF3) can be found as a function of applied field and temperature in HoB_{12}. For a field applied in the crystallographic (111) and (110) directions, all three magnetic phases seem to merge in one point close to T_N=7.4 K; i.e., in this point, all three phases should coexist. The critical field is certainly below 0.5 T, but based on the magnetization data it was not possible to achieve an improved estimate for the multicritical point(s). For the orientation (100) the phase boundary between phases AF2 and AF3 at low magnetic field cannot be determined unambiguously as the magnetization data in this case do not exhibit sharp and well-distinguishable kinks.

The observed heat capacity $C(T)$ is displayed in Fig. 3. In zero magnetic field a very steep increase at

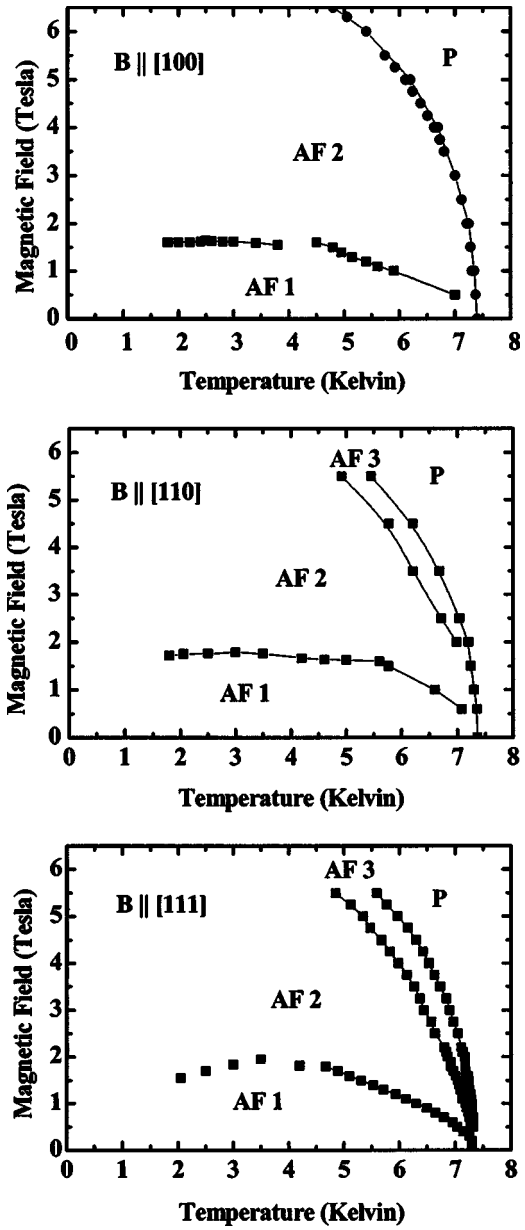

FIG. 2. Phase diagram of HoB_{12} as a function of magnetic field and temperature for fields applied along the (100), (111), and (110) directions. Lines are drawn to guide the eye. Most of the data points were obtained from temperature scans, except for the flat parts of the boundary between the AF1 and AF2 phases which are derived from scans of the magnetic field at constant temperature.

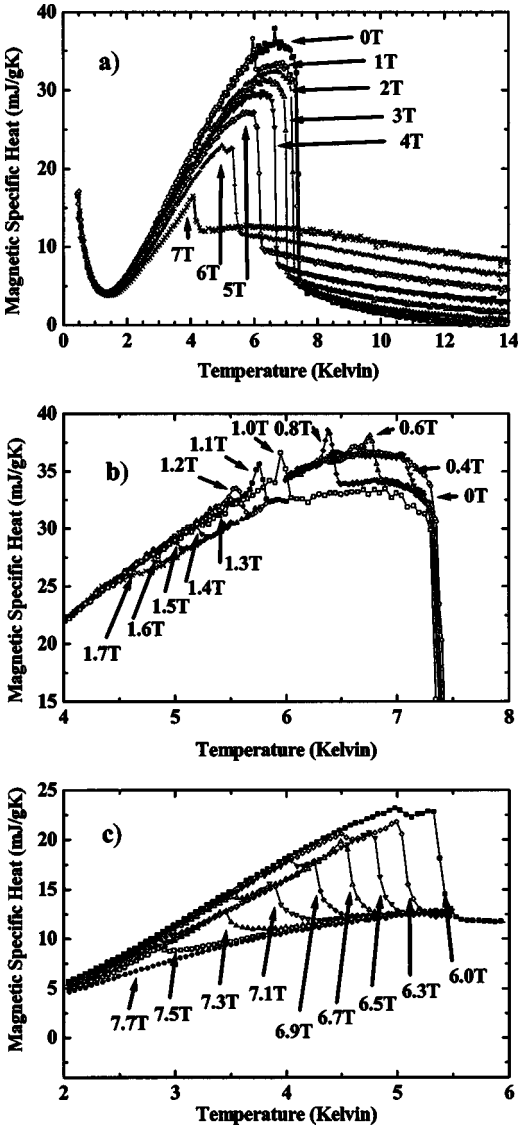

FIG. 3. Specific heat as a function of temperature, measured on a single-crystal HoB_{12} sample of 8.8 mg mass. The field was applied parallel to the (100) axis of the sample. The lattice contribution was estimated from the measured $C(T)$ around 30 K and has been subtracted, assuming a T^3 temperature dependence. (a) gives an overview of the measured data; (b) and (c) show the evolution of the specific heat in the low-field and high-field regimes in more detail.

$T_N=(7.40\pm0.02)$ K can be seen, but the maximum of $C(T)$ is reached only at temperatures around 6.6–6.8 K. The steep increase at T_N may be taken as an indication of a first-order phase transition. However, no hysteresis of $C(T)$ is observed in our experiments and the entropy calculation does not show any jump at T_N as well. The behavior at T_N may best be seen in the thermal relaxation following a heat pulse (Fig. 4): the $T(t)$ trace can well be described with exponential relaxation functions. At T_N a sharp change of the time constant is observed, showing first of all that the phase transition is very sharp and the uncertainty of T_N from the fits to the exponential decay is less than $\Delta T_N=5$ mK. From the amount of heat transferred to the heat bath during the time of nonexponential relaxation the upper bound for the latent heat was estimated to be about 6 μJ/g.

In the paramagnetic region of HoB_{12} at about 40 K a Schottky contribution to the specific heat is observed.[15] This was interpreted to suggest an important role of the crystalline electric field on the physical properties of this compound above T_N. From these results it was also shown that the ground state of HoB_{12} is the $\Gamma_5{}^1$ with a splitting of ~416 K. From entropy calculations it follows that the ordered ground state can be described with an effective angular momentum $J=1$.

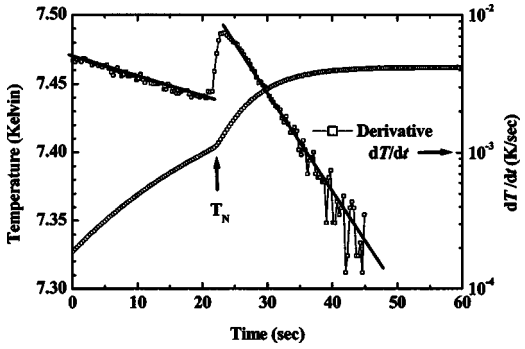

FIG. 4. Temperature relaxation profile of the calorimeter after a 1% increase of the applied heater power at $T_0 = 7.32$ K. The derivative was calculated numerically and is displayed on a logarithmic (right) scale. It is evident that the relaxation is exponential; the inverse slopes of the straight lines (i.e., the time constants) below and above $T_N = 7.40$ K are directly proportional to the corresponding specific heat. Deviations from exponential relaxation occur around T_N in a very limited time interval of less than 5 s which corresponds only to a few mK temperature change. These deviations have been used to determine an upper bound for the latent heat for a possible first-order phase transition. These deviations, however, may as well be caused by experimental artifacts like sample size effects.

The magnitude of the heat capacity discontinuity at T_N and the shape of $C(T)$, in particular the fact that the maximum is reached well below T_N, are features typical of incommensurate amplitude-modulated magnetic structures.[19,20] In this structure the magnetic moment amplitude varies periodically with a wave vector which does not correspond to a symmetry point of the Brillouin zone.

With a magnetic field parallel to the crystallographic orientation (100) the overall heat capacity picture remains very similar, but the steep increase of $C(T)$ at T_N gets reduced in amplitude. Moreover, with an increase of the magnetic field of between about 0.4 T and 2 T a sharp peak in the $C(T)$ dependence is observed. A detailed picture of the evolution of this peak, which vanishes above 2 T, is shown in Fig. 3(b). The integration of the specific heat shows that the entropy change associated with these peaks is very small. Between about 4 T and 8 T another peak in the heat capacity dependence can be seen [see Fig. 3(c)], which points to the phase boundary between phases AF2 and AF3 observed in the magnetization experiment.

At the lowest temperatures, in addition, a contribution from the hyperfine enhanced ^{165}Ho nuclear moments is observed [cf. Fig. 3(a)]. However, the expected temperature and magnetic field dependence of this contribution, which should scale as $(B/T)^2$, was not seen. Instead, a $(B/T)^{3/2}$ dependence was found. The reason for this deviation is likely connected with the variation of the electronic magnetization M which changes as a function of both T and B and thus modifies the local field $B_{loc} \sim AM$ seen by the nuclei where A is the parameter of the hyperfine exchange interaction.

The results from the specific heat experiment were used to construct a phase diagram with three phases in an applied magnetic field (Fig. 5). This phase diagram compares very well with that based on magnetization data (Fig. 2). For the

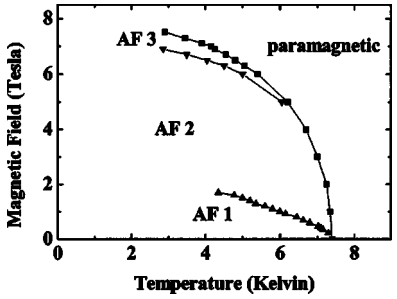

FIG. 5. Phase diagram derived from specific heat measurements on a HoB_{12} single crystal with a magnetic field applied parallel to the (100) axis. Note the phase boundary between the phases AF2 and AF3 which has not been observed in the magnetization experiments.

crystallographic direction (100) it shows that in this direction the phase boundary between phases AF2 and AF3 does not join at T_N as is the case for the (111) and (110) directions, but at lower temperature and in a nonzero magnetic field. The phase boundary lines between the paramagnetic and antiferromagnetic (P and AF1/AF3) phases follows well the relation $(B/B_C)^2 + (T/T_C)^2 = \text{const}$.

The observed magnetic phase diagram of HoB_{12} (Figs. 2 and 5) is quite complex; it represents an interesting problem with respect to all the reasons leading to its formation. The comparison to HoB_6, which crystallizes in the bcc symmetry with a Γ_5^2 ground state, may be useful. HoB_6 was shown to exhibit a standard λ-like antiferromagnetic transition at 5.6 K (Refs. 21 and 22). As the ground states of HoB_{12} (Γ_5^1) and HoB_6 are similar and both exhibit a threefold ground-state degeneracy, it appears that different interactions and the different crystal symmetry lead to the various magnetic phases in HoB_{12}. In particular, the interplay between RKKY and dipole-dipole interactions could be one reason for the striking difference to HoB_6; another reason could be the frustration of the fcc lattice.

To shed more light on the magnetic structure of HoB_{12}, neutron diffraction investigations of an isotopically enriched powder sample were carried out at temperatures above and below T_N and in a magnetic field up to 5 T. The diffraction pattern at 1.7 K and the difference of powder spectra obtained at temperatures below and above T_N and in zero magnetic field are shown in Fig. 6.

The neutron data can be understood assuming an incommensurate magnetic structure with a propagation vector $q = (1/2 - \delta, 1/2 - \delta, 1/2 - \delta)$, where $\delta = 0.035$. The applicability of this representation can be seen in Fig. 6—all of the observed positions are matched well. Comparing the indexing for reflections (Fig. 7) it is obvious that, e.g., $(3/2 \pm \delta, 3/2 \pm \delta, 3/2 \pm \delta)$ and $(5/2 \pm \delta, 1/2 \pm \delta, 1/2 \pm \delta)$ are higher-order reflections to the propagation vectors $\pm(1/2 - \delta, 1/2 - \delta, 1/2 - \delta)$. Vice versa, mixed reflections like $(3/2 \pm \delta, 1/2 \pm \delta, 1/2 \pm \delta)$ and $(3/2 \pm \delta, 3/2 \pm \delta, 1/2 \pm \delta)$ come from different domains of the ordering vector parallel to the (-111) and $(-1-11)$ directions, respectively.

While the ordering vector is well defined, it is more difficult to determine the spin structure. An attempt was made to refine a sinusoidal amplitude-modulated moment arrange-

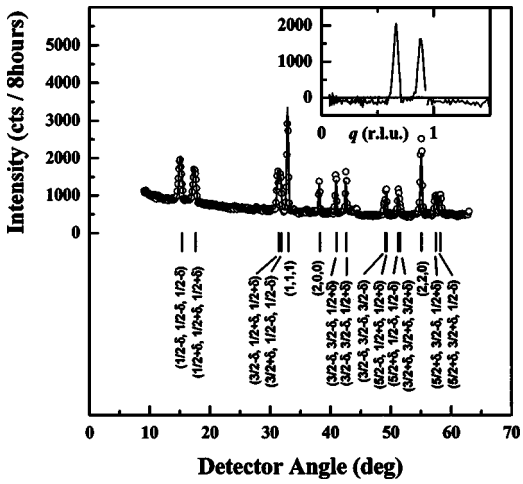

FIG. 6. Powder diffraction pattern measured on a polycrystalline Ho $^{11}B_{12}$ sample at 1.7 K in a zero magnetic field. Circles are measured data points; the line corresponds to the fit for an amplitude-modulated structure. Except for the structural (111), (200), and (220) reflections which remain independent of temperature all other reflections disappear above 7.4 K. The inset shows the difference between scans taken at 1.7 K and 15 K for the fundamental reflections as function of the momentum transfer. Note the reduction of the background at low temperature seen in the difference plot.

ment and a spiral structure. In the absence of more information an equal distribution of magnetic domains has been assumed. In case of the spiral structure the fit has not been satisfactory. The amplitude-modulated structure with a collinear arrangement of moments perpendicular to the ordering vector was a significant improvement (cf. Fig. 6) compared to a magnetic spiral. The remaining error can well be attributed to experimental difficulties which were connected with the need to change the detector position and to a slight texture of the powder sample.

Not only because the refinement of the collinear amplitude-modulated structure was better than the spiral, it is interesting to consider this case more seriously: it is consistent with the specific heat data because amplitude-modulated structures are expected when the specific heat shows a maximum below the Neél temperature.[20] The variation of the moment along a space diagonal (Fig. 8) shows that in that case a significant part of the magnetic moments remains disordered. At low temperature, squaring of amplitude modulated structures is expected[20] and higher harmonics should appear. However, they are not observed in the powder experiment.

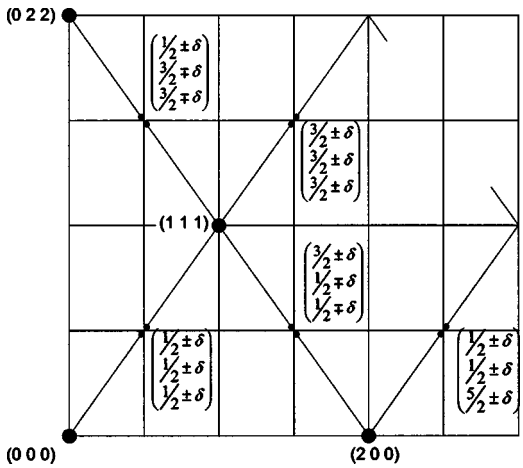

FIG. 7. Reciprocal space map of the observed reflections. The $(5/2\pm\delta, 3/2\mp\delta, 1/2\pm\delta)$ reflections, which have been observed as well, are not seen in this projection.

FIG. 8. Moments for an amplitude-modulated structure on the fcc lattice along the (111) axis. Following the refinement, the moments are perpendicular to the ordering vector [here $q=(1/2-\delta\,1/2-\delta\,1/2-\delta)$]. Within successive (111) planes the moments are parallel. Note that the average moment is reduced in this model; the remaining part of the moment is disordered.

In fields of 1 T and 1.5 T the intensity of the antiferromagnetic reflections increases smoothly as a function of temperature between $T_N=7.4$ K and about 4 K. No jumps are observed, which points to a continuous (second-order) phase transition at T_N, in agreement with the specific heat results. Below approximately 4 K the increase becomes steeper with decreasing temperature. The reasons for this behavior are not clear.

Scans at various temperature in magnetic fields between 0 and 5 T were carried out in order to see whether there are indications for phase boundaries between antiferromagnetic phases. The principal reflections remain; i.e., no change in the antiferromagnetic propagation vectors in low magnetic field was observed. In Fig. 9 the results are summarized: The intensity of the basic reflection at $(1/2\pm\delta, 1/2\pm\delta, 1/2\pm\delta)$ reduces significantly in fields higher than 2 T. The mixed reflections $(3/2\pm\delta, 1/2\mp\delta, 1/2\mp\delta)$ close to (111) are much less affected by the external field. A likely reason for these observation is the repopulation of magnetic domains in an applied field. Parallel to the reduction of antiferromagnetic reflections the structural (111) reflection increases in fields above 2 T because a ferromagnetic moment in the field direction is developing. In a 5-T field we estimate a moment of

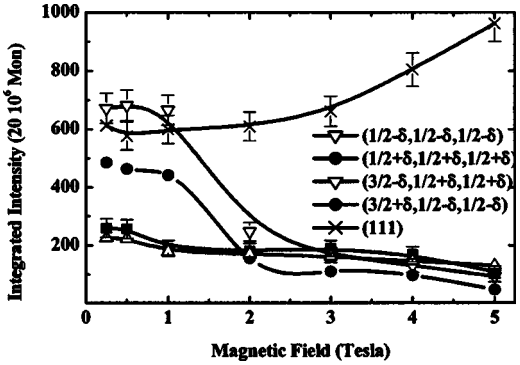

FIG. 9. Magnetic field dependence of some reflection intensities measured at 1.7 K. The lines are guides to the eyes; error bars are based on the counting statistics.

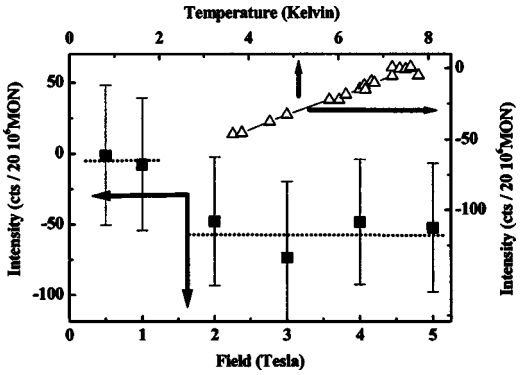

FIG. 10. Change of the magnetic background signal as a function of magnetic field (left/bottom axis, solid symbols). For comparison, the background variation as a function of temperature in a zero field has been added using the same scaling factors for the intensities (open symbols, top right axis).

$3.4\mu_B$ in reasonable agreement with the magnetization data (cf. Fig. 1) where $3\mu_B$ is found in a 5-T field. The changes of the neutron scattering data, both as a function of temperature and field, correlate well with the location of the phase boundaries found in the specific heat and magnetization experiment (Fig. 5), thus confirming the phase boundary inferred from specific heat data.

The behavior of the background was surprising: in zero field it decreases below T_N as the temperature is reduced. This is expected because the paramagnetic diffuse signal decreases as the antiferromagnetic reflections grow. The field dependence measured well within the ordered phase at $T=1.7$ K shows that the background reduces further in applied fields. In a 5-T field the change of background compares well to the amount observed in zero field as a function of temperature (Fig. 10). This can only be possible if in zero field, even at a fairly low temperature compared to T_N, a significant amount of disorder remains which disappears only in an applied field. This finding is in accordance with the amplitude-modulated structure discussed above. Thus, the diffuse signal (originating from disordered magnetic moments) further supports this model. With the present data, although the number of measured field points is not large, it is tempting to characterize the zero-field phase below the 2-T field as an incommensurate structure with a significant amount of disorder.

IV. CONCLUSIONS

We can conclude that HoB_{12} exhibits a quite complex magnetic phase diagram as a function of temperature and applied magnetic field. Powder neutron diffraction in a zero magnetic field likely reveals an incommensurate amplitude-modulated magnetic structure below T_N, the basic reflections can be indexed by $(1/2\pm\delta,1/2\pm\delta,1/2\pm\delta)$, where $\delta=0.035$. The present data show three phases in an applied field. Within experimental resolution the phase boundaries of all phases merge close to zero field at T_N, except for $B\|$ [100] where only the AF1 and AF2 phase boundaries merge at T_N. This is remarkable because then at T_N different phases and therefore different structures should coexist. Both the AF1 and AF2 phases can be characterized by the same incommensurate ordering vector. The difference between both phases is the observation of a ferromagnetic moment in the field direction in the AF2 field phase and the striking observation that in the zero-field phase a significant amount of the moment remains disordered. The latter observation supports an incommensurate amplitude-modulated structure and seems to be in qualitative agreement with recent observation of Kalvius *et al.*[23] using muon spin rotation techniques. Such a structure is supported further by the fact that the maximum of the specific heat is reached only below T_N.

The steep increase of the specific heat at T_N might suggest a first-order phase transition. However, the upper bound for the latent heat is very low and therefore the transition could only weakly be of first order. Without exact knowledge of the magnetic structure also other features of the specific heat are difficult to analyze. In particular the model of Blanco *et al.*,[20] which nicely explains the maximum of the specific heat below T_N with an amplitude-modulated structure, is not directly applicable because it predicts squaring. This cannot be confirmed by the present neutron data because higher harmonics are not observed.

Finally, we should compare to the nuclear spin system of Cu. The experimental results—as far as the phase diagram is concerned—confirm the picture that both cases are similar. Three AF phases are found as a function of magnetic field and entropy (temperature). It is interesting that even the topology of the phase diagram is reproduced, in Cu, and the phases seem to merge at a critical entropy (the entropy is a "good" thermodynamic variable for the isolated nuclear spin system). In HoB_{12}—as mentioned above—the phase boundaries also meet close to T_N. It is therefore reasonable to assume that the dipolar interaction is the reason for the complex phase diagram of this compound because no other anisotropy should be present: the cubic crystal field is namely not effective for $J=1$. Strain-induced quadrupolar anisotropy has been investigated in the paramagnetic state and was found to be negligible.[15]

The comparison between the antiferromagnetic structure of these systems, however, is less favorable because in the case of HoB_{12} an incommensurate ordering vector is observed which does not change with magnetic field in the various phases whereas the nuclear ordering of Cu has shown commensurate structures[16] within the three AF phases. Nevertheless, in Cu a similar problem was encountered between the zero-field and high-magnetic-field phases which both order with $q=(100)$. As pointed out by Lindgård,[18] the interplay between interactions in the ordered state as a function of magnetic field leads to a different canting of moments which distinguishes the phases. This could well be imagined also for the case of HoB_{12}, although with the present powder data it is not possible to sort out possible moment reorientation transitions.

The incommensurate structure of HoB_{12} compares to the intermediate field phase of copper which is characterized by $q=(0,2/3,2/3)$. In the case of Cu it was namely predicted that this structure is close to stability through the interplay of the RKKY and dipolar interactions with an incommensurate

ordering vector which only depends on the ratio of both interactions.[18] These arguments certainly can be transferred to the case of HoB_{12}. The amplitude modulation suggested for HoB_{12} finds another interesting correspondence in an alternative suggestion for the stability of the (0, 2/3, 2/3) phase in Cu at a finite magnetic field. Similar to Blanco *et al.*,[20] in a variational approach by Oja *et al.*[17] it was assumed that the moments could be modulated. There, however, only a structure with equal moments was stable in an external field and this structure "accidentally" was the commensurate (0, 2/3, 2/3) type.

Thus a detailed explanation of the present results clearly requires more knowledge of the magnetic structure, especially of the individual phases. Nevertheless, the present work shows that the RB_{12} system is very suitable to test theories of antiferromagnetic ordering in fcc symmetry, to characterize the role of various interactions and the possible implications from the frustration of the AF ground state.

ACKNOWLEDGMENTS

This work was supported by the EC through Access to Research Infrastructures actions of Human Potential Programme under the 5th Framework Program (CT RTN 2000 00166), by the German exchange agency DAAD, by the Slovak Scientific Grant Agency VEGA, Contract Nos. 4061 and 3195, and by the INTAS Project, Ref. No. 03-51-3036.

[1] J. Etourneau and P. Hagenmuller, Philos. Mag. B **52**, 589 (1985).
[2] M. Kasaya, F. Iga, M. Takigawa, and T. Kasuya, J. Magn. Magn. Mater. **47&48**, 429 (1985).
[3] I. Bat'ko, M. Bat'ková, K. Flachbart, V. B. Filipov, Yu. B. Paderno, N. Yu. Shitsevalova, and Th. Wagner, J. Alloys Compd. **217**, L1 (1995).
[4] H. Ohta, T. Nanba, K. Lehnert, S. J. Allen, M. Motokawa, F. Iga, and M. Kasaya, J. Magn. Magn. Mater. **177–181**, 341 (1998).
[5] S. Gabáni, I. Bat'ko, K. Flachbart, T. Herrmannsdörfer, R. König, Y. Paderno, and N. Shitsevalova, J. Magn. Magn. Mater. **207**, 131 (1999).
[6] K. E. Spear, in *Boron and Refractory Borides*, edited by V. I. Matkovich (Springer, Berlin, 1977), p. 439.
[7] H. C. Longuet-Higgins and M. de Roberts, Proc. R. Soc. London, Ser. A **224**, 336 (1954).
[8] H. C. Longuet-Higgins and M. de Roberts, Proc. R. Soc. London, Ser. A **230**, 110 (1955).
[9] W. N. Liscomb and D. Britton, J. Chem. Phys. **33**, 275 (1960).
[10] H. Harima, A. Yanase, and T. Kasuya, J. Magn. Magn. Mater. **47&48**, 567 (1985).
[11] H. Harima, A. Yanase, Y. Onuki, I. Umehara, Y. Kurosawa, Y. Nagai, K. Satoh, T. Kasuya, and F. Iga, Physica B **165&166**, 343 (1990).
[12] M. Heinecke, K. Winzer, J. Noffke, H. Grieb, K. Flachbart, and Yu. B. Paderno, Z. Phys. B: Condens. Matter **98**, 231 (1995).
[13] L. L. Moiseenko and V. V. Odintsov, J. Less-Common Met. **67**, 237 (1979).
[14] P. C. M. Gubbens, A. M. van der Kraan, and K. H. J. Buschow, Physica B & C **130**, 412 (1985).
[15] N. Shitsevalova, Ph.D. thesis, University of Wroclaw, Poland, 2001; A. Kohout, Ph.D. thesis, Technical University of Berlin, 2003.
[16] A. J. Annila, K. N. Clausen, P.-A. Lindgard, O. V. Lounasmaa, A. S. Oja, K. Siemensmeyer, M. Steiner, J. T. Touriniemi, and H. Weinfurter, Phys. Rev. Lett. **64**, 1421 (1990).
[17] A. S. Oja and O. V. Lounasmaa, Rev. Mod. Phys. **69**, 1 (1997).
[18] P. A. Lindgard, Phys. Rev. Lett. **61**, 629 (1988).
[19] M. Bouvier, P. Lethuillier, and D. Schmitt, Phys. Rev. B **43**, 13 137 (1991).
[20] J. A. Blanco, D. Gignoux, and D. Schmitt, Phys. Rev. B **43**, 13 145 (1991).
[21] K. Segawa, A. Tomita, K. Iwashita, and S. Kunii, J. Magn. Magn. Mater. **104–107**, 1233 (1992).
[22] S. Kunii, K. Takahashi, and K. Iwashita, J. Solid State Chem. **154**, 275 (2000).
[23] G. M. Kalvius, D. R. Noakes, M. Marcano, R. Wapping, F. Iga, and T. Takabatake, Physica B **326**, 398 (2003).